

Corrosion mitigation of mild steel in simulated concrete pore solution using henna seed extract as a green inhibitor

Pooviah Shanthy¹, Murugesan Sindhu¹, Susai Rajendran^{2,3,*} , Abdulhameed Al-Hashem⁴

¹ Department of Chemistry, Sri Meenakshi Government Arts College for Women (Autonomous), Madurai 625002, India

² Department of Chemistry, Corrosion Research Centre, St. Antony's College of Arts and Sciences for Women (Autonomous), Dindigul 624005, India

³ St Antony's College, Mother Teresa Women's University, Kodaikanal 624101, India

⁴ Petroleum Research Centre, Kuwait Institute for Scientific Research, Kuwait City 13109, Kuwait

* Corresponding author: Susai Rajendran, susairajendran@gmail.com

CITATION

Shanthy P, Sindhu M, Rajendran S, et al. Corrosion mitigation of mild steel in simulated concrete pore solution using henna seed extract as a green inhibitor. *Building Engineering*. 2026; 4(1): 3892.
<https://doi.org/10.59400/be3892>

ARTICLE INFO

Received: 5 November 2025

Revised: 17 December 2025

Accepted: 19 December 2025

Available online: 13 January 2026

COPYRIGHT



Copyright © 2026 Author(s).
Building Engineering is published by Academic Publishing Pte. Ltd. This work is licensed under the Creative Commons Attribution (CC BY) license. <https://creativecommons.org/licenses/by/4.0/>

Abstract: Corrosion in concrete structures presents a significant challenge that affects their safety, durability, and structural integrity, primarily due to environmental factors and chemical reactions. An aqueous extract derived from henna seed has been utilized to mitigate the corrosion of mild steel in a simulated concrete pore solution (SCPS). A study on polarization has been conducted to assess the corrosion protection properties of henna seed extract (HSE). The addition of henna seed extract leads to an enhancement in linear polarization resistance. Conversely, there is a decrease in the corrosion current. In the presence of henna seed extract, the linear polarisation resistance of mild steel in simulated concrete pore solution increases from 750 Ohm cm² to 1198 Ohm cm². The corrosion current value decreases from 6.719×10^{-5} A/cm² to 2.925×10^{-5} A/cm². The surface morphology of the protective film has been examined using scanning electron microscopy (SEM). It has been noted that when henna seed extract is present, the surface of the protective film exhibits a smoother texture. These findings confirm the corrosion protection offered by henna seed extract. An additional investigation into contact angle measurements indicates that when henna seed extract is present, the protective film developed on the surface of mild steel, which is immersed in simulated concrete pore solution (SCPS), exhibits a comparatively smoother texture. The resistance to corrosion is enhanced. This aligns with the findings from the electrochemical investigation, specifically the polarization study, as well as the images obtained from scanning electron microscopy (SEM). These results could have implications in the field of concrete technology.

Keywords: corrosion control; mild steel; simulated concrete pore solution; extract of henna seed; green inhibitors

1. Introduction

Corrosion in concrete structures poses a considerable challenge that impacts their safety, durability, and structural integrity, mainly due to environmental influences and chemical reactions. Factors contributing to corrosion encompass chloride attack, carbonation, moisture, and fluctuations in temperature. Chlorides, which are frequently sourced from de-icing salts or marine settings, infiltrate the concrete and compromise the protective oxide layer on steel reinforcement, resulting in the development of rust. Carbonation denotes the chemical process that involves carbon dioxide, leading to the creation of carbonates, bicarbonates, and carbonic acid. Elevated moisture levels in

concrete can hasten corrosion processes, since water is crucial for the electrochemical reactions that contribute to rust formation. Variations in temperature can lead to the emergence of stress cracks in concrete, which facilitates the easier penetration of corrosive substances. A multitude of studies have been carried out to address the corrosion of rebars embedded in concrete structures. In these research efforts, a simulated concrete pore solution (SCPS) has been employed. Generally, SCPS is composed of a saturated solution of calcium hydroxide [1–5]. Calcium oxide [6–10] can also be used as a simulated concrete pore solution.

Carry et al. [1] conducted a study on the HS2 high-speed line, focusing on the supply and qualification of an electrically isolated prestressing system that adheres to the fib 75 standards for a viaduct constructed with prefabricated segments.

The method of prestressing concrete structures allows for various optimizations in structural design, such as minimizing the size of concrete and steel elements and improving span lengths.

Consequently, the durability of steel tendons, which are continuously tensioned to maintain prestressing forces, is crucial for the stability of these structures.

Moreover, the stress applied to these tendons, approximately 90% of their elastic limit during the construction phase, along with their exceptional mechanical strength, necessitates protection against corrosion processes, particularly stress corrosion.

Freyssinet manages the production, supply, and project management support for the installation of these prestressing tendons used in the prefabricated segment structures associated with the HS2 project [1].

The assessment of non-destructive methods for examining post-tensioned concrete bridges has been conducted by Rossi et al. [2]. Bridges constructed with reinforced concrete and equipped with post-tensioned (PT) cables are especially critical structures, as the deterioration of the tendons cannot be completely detected through traditional investigation techniques and/or visual evaluations, owing to the distinctive characteristics of this type of structure. Indeed, PT cables are contained within plastic or metal conduits designed to shield them from corrosion.

However, this also conceals them, rendering it impractical to assess their condition solely through visual inspection. The deterioration of PT systems is generally classified into strand defects and grout defects. The objective is to furnish bridge owners with a decision-making tool that can aid them in selecting the most suitable non-destructive technology for evaluating a specific strand or grout defect [2].

The utilization of embedded sensor technology within the offshore energy sector has been examined by Allady and Maini [3]. For a considerable duration, offshore structures have acted as the cornerstone of the energy industry. Nevertheless, uncertainties remain concerning the degree to which strain, displacement, settlement, and other variables affect the different elements of offshore structures. How are these variables validated and evaluated against design loads? Are mathematical and finite element methods the only techniques utilized? With the swift advancement of sensor technologies, leaders in the offshore energy sector have, out of necessity, started to adopt sophisticated solutions such as Smart Structures' Embedded Data Collectors (EDCs) for reinforced concrete pile foundations, alongside sensor technology for

monitoring external contact on steel components.

The potential for expanding the application of EDC technology, presently utilized in surface transportation infrastructure, to the offshore energy sector has been investigated. It highlights various benefits linked to real-time [3].

The advanced modeling of concrete structures aimed at enhancing sustainability has been examined by Rymeš et al. [4]. One approach to strengthen the sustainability of the concrete sector is to ensure the safe and long-lasting serviceability of concrete structures. This research introduces a pilot implementation of a holistic system designed for the online monitoring and forecasting of the service life of concrete bridges. The system comprises strain gauges that evaluate the structural response, in addition to a laser rangefinder that detects traffic crossing the bridge.

The collected data were utilized to develop a computational model of the bridge. Subsequently, deterioration models were incorporated into the model to evaluate the long-term mechanical performance. This research focused on chloride-induced corrosion of the reinforcement. Numerical data are provided for a service life prediction spanning a duration of 100 years [4].

The evaluation of the structural integrity of submerged concrete structures through quantitative non-destructive techniques implemented via remotely operated underwater vehicles (ROV) has been conducted by Venkatesh et al. [5]. Marine assets located in ports, harbors, and those integrated into our civil infrastructure, such as dams and bridges, experience ongoing structural degradation over time. Numerous national and international disasters in recent years have demonstrated that these aging infrastructures present significant risks from both social and economic viewpoints.

Consequently, regular assessments of marine assets are crucial for the timely detection of deterioration, the organization of maintenance tasks, and the formulation of restoration strategies designed to extend their lifespan, avert significant damage, and safeguard lives.

Non-destructive testing of concrete structures is conducted through various methods, including ultrasonic tomography, ground penetrating radar, and radiography, to identify structural irregularities and evaluate the remaining lifespan.

The findings presented in this study will prove advantageous to asset owners and managers, allowing them to make informed decisions grounded in inspection results [5].

A life cycle assessment from cradle to gate of CFRP reinforcement for concrete structures has been conducted by Stoiber et al. [6]. The construction industry significantly contributes to global CO₂ emissions, with concrete, particularly its binder cement, accounting for a substantial portion. Therefore, it is essential to investigate solutions that minimize the quantity of concrete utilized in construction.

One potential method involves the use of carbon fiber-reinforced polymers (CFRP) for reinforcement, alongside sophisticated structural design techniques that focus on minimizing the size and consequently the weight of concrete building elements. CFRP reinforcement is acknowledged for its outstanding tensile strength and advantageous corrosion resistance in comparison to traditional steel reinforcement.

Nonetheless, the manufacturing of carbon fibers requires considerable resources and energy. This research study assesses the environmental effects of CFRP

reinforcement in concrete structures, considering the present state of data availability and standardization. A cradle-to-gate life cycle assessment is performed [6].

The management of concrete temperature through the alternating use of post-cooling or pre-cooling (utilizing liquid nitrogen) during the construction of the “Puente del Atlantico” in Panama has been executed by Ladouceur et al. [7]. Throughout its lifespan, a structure must withstand different forms of stress or loading, which may include physical, mechanical, or chemical forces, while maintaining its overall durability and aesthetic appeal to the utmost extent. The durability of the structure must be confirmed by adhering to a series of technical recommendations within a regulatory framework.

Among these guidelines, in addition to those addressing rebar corrosion issues, special emphasis should be placed on improving the management of concrete’s thermal behavior. This is crucial to avert both self-induced expansions (i.e., Delayed Ettringite Formation) and significant temperature differentials within the structure, which could heighten the risk of early-age thermal cracking. Such cracking has been shown to significantly affect the service life management of a structure.

This study outlines the comprehensive strategy employed by the Contractor in the construction of a significant cable-stayed bridge and its accompanying viaducts in Panama, aimed at addressing thermal issues within the local environment [7].

Heffron has performed a study on numerical modeling aimed at enhancing the durability of concrete for newly constructed waterfront structures intended to last for a century or longer [8].

The process of designing for concrete durability does not have to be enigmatic. Numerous technologies and products are currently available in the market that can meet durability objectives of 100 or even 200 years. However, it is essential to address the following key questions:

1. What is the associated cost?
2. How can we guarantee that these targets are attainable?
3. What quality control measures are necessary to achieve these goals?

The United States Navy has assumed a prominent position in the development of sophisticated modeling techniques for concrete durability, with the objective of protecting its significant investments in new waterfront infrastructure. This technology is accessible to everyone and is presently being employed in commercial waterfront projects. Thanks to progress in numerical modeling techniques, it is now feasible to quantitatively forecast durability with a considerable level of precision [8].

Muñoz and Valbuena have conducted a State assessment of steel bridges within the Colombian National roadway network [9]. This document provides a comprehensive analysis of the state assessment and common damages associated with steel and composite structures (concrete combined with steel) in the National Roadway Network, excluding seismic evaluations. The study is based on the inventory and inspections carried out by the Colombian Government’s Roads Institute (Invias) since 1996, employing the Colombian Bridge Management System (Sipucol).

This document is organized into two parts: the initial part presents a brief summary of the different categories of steel bridges and composite structures as detailed in the

Sipucol inventory module, whereas the latter part offers an in-depth analysis of the state and common damages affecting the main components. Within the National Roadway Network, there are 244 steel and composite structure bridges that exhibit structural deficiencies, which include both widespread and localized corrosion, issues related to water infiltration, insufficient joint details, the occurrence of fatigue problems in the joints, and substandard quality in welded joints [9].

Silver has conducted a study titled “Bridge steps lightly to spare cash crop” [10]. This report discusses the reconstruction project of a bridge that crosses Apalachicola Bay, noted as the largest area for oyster bed production. The new bridge consists of two components: the lower causeway, which is 3 miles long and has a minimum clearance of 14 feet above the water, and the upper section, providing a vertical clearance of 65 feet from the water.

This newly built prestressed concrete bridge features two traffic lanes along with two breakdown lanes. The project adheres to the regulations established by the Florida Department of Transportation and incorporates environmental considerations by utilizing 54-inch diameter piles, thereby reducing disturbances to the seabed of the bay. The design team has worked in conjunction with local fishermen to assist in relocating the oyster beds located directly beneath the piles. Additionally, a portion of the causeway has been maintained to function as a bird sanctuary [10].

2. Experiments

2.1. Henna seed

In the current study, an aqueous extract obtained from henna seed has been employed to reduce the corrosion of mild steel in a simulated concrete pore solution (SCPS). A polarization analysis has been performed to evaluate the corrosion protection efficacy of the henna seed extract (HSE) [11].

Henna seed (**Figure 1**) originate from the *Lawsonia inermis* plant, a tropical shrub that flourishes in warm climates. This plant is greatly esteemed for its leaves, which are utilized to produce henna dye, a favored option for temporary tattoos and hair coloring. Henna carries profound historical importance, tracing back to ancient Egypt, and is extensively employed in numerous cultures for body art and ceremonial functions.

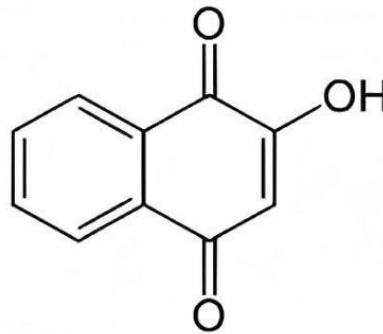


Figure 1. Henna seed.

2.2. Chemistry of henna seed

The composition of henna seed, particularly those sourced from the henna plant (*Lawsonia inermis*), includes lawsone, a reddish-orange pigment that interacts with

keratin found in skin and hair, leading to a long-lasting stain. Lawsone (**Figure 2**), which is a derivative of hydroxyquinone, is recognized for its potent staining properties.



Lawsone (2-Hydroxy-1,4-naphthaquinone)

Figure 2. Structure of Lawsone.

2.3. Preparation of simulated concrete pore solution (SCPS)

In the present study, a saturated calcium hydroxide solution is employed as the SCPS solution. The pH was recorded at 13.5.

2.4. Inhibitor

30 g of dried henna seed are measured, finely ground with 20 mL of water, and then filtered. The resulting filtrate is adjusted to a total volume of 100 mL in a 100 mL standard measuring flask using ground water.

2.5. Preparation of specimen

Mild steel samples (0.15% C, 0.18% Si, 0.45% Mn, 0.03% S, and the remainder iron) measuring $1.0 \times 4.0 \times 0.2$ cm were polished to achieve a mirror-like finish, degreased using trichloroethylene, and utilized for surface examination studies.

2.6. Electrochemical study

The corrosion resistance of mild steel has been assessed using an electrochemical analysis referred to as the Polarization study.

3. Results and discussion

3.1. Polarisation study

An electrochemical workstation, model 660A from CHI, was used for this research. A three-electrode cell assembly was implemented in the current study (see **Figure 3**). Mild steel was utilized as the working electrode, while a saturated calomel electrode served as the reference electrode, and a platinum electrode was also incorporated. The polarization study allowed for the determination of corrosion parameters, including corrosion potential (E_{corr}), corrosion current (I_{corr}), Tafel slope values (anodic = b_a and cathodic = b_c), and linear polarization resistance (LPR).

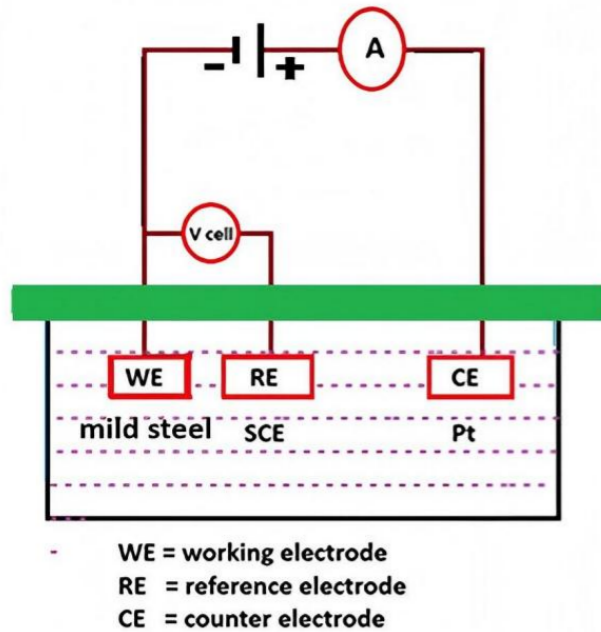


Figure 3. Three electrode cell assembly.

The examination of polarization has been utilized to detect the formation of a protective layer on the surfaces of metals. When a protective layer is formed on the metal surface, the linear polarization resistance (LPR) increases, whereas the corrosion current (I_{corr}) decreases (**Figure 4**) [12–16].

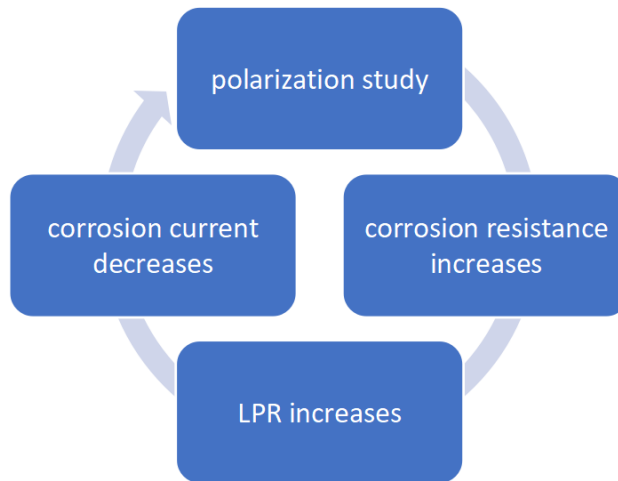


Figure 4. Correlation among corrosion parameters of the Polarisation study.

The potentiodynamic polarization curve for mild steel immersed in various test solutions is depicted in **Figure 5**. The corrosion parameters, namely the corrosion potential (E_{corr}), Tafel slopes (b_c = cathodic; b_a = anodic), linear polarization resistance (LPR), and the corrosion current (I_{corr}), are detailed in **Table 1**.

Table 1. Corrosion parameters of mild steel submerged in various test solutions.

System	E_{corr} mV vs. SCE	b_c mV/decade	b_a mV/decade	LPR Ohm cm^2	I_{corr} A/ cm^2
SCPS	-579	200	275	750	6.719×10^{-5}
SCPS + HSE	-734	172	152	1198	2.925×10^{-5}

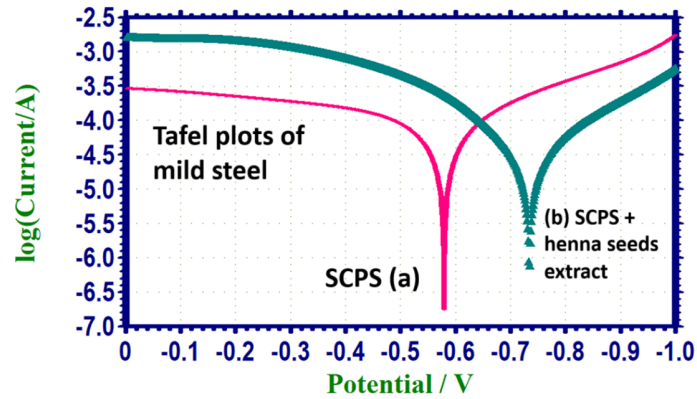


Figure 5. Potentiodynamic Polarization curves of mild steel immersed in various test solutions. Note: (a) SCPS; (b) SCPS + henna seed extract.

3.2. Mild steel in SCPS

When mild steel is immersed in SCPS, the corrosion potential is -579 mV vs SCE. The LPR value is $750 \text{ Ohm}\cdot\text{cm}^2$. The corrosion current is $6.519 \times 10^{-5} \text{ A/cm}^2$.

3.3. Influence of henna seed extract on the corrosion resistance of mild steel immersed in SCPS

The formulation containing an extract of henna seed alters the corrosion potential from -579 to -734 mV relative to SCE. This shift in corrosion potential moves towards the cathodic side, indicating that the cathodic reaction is primarily controlled.

The LPR value increases from 750 to $1198 \text{ Ohm}\cdot\text{cm}^2$, and the corrosion current decreases from 6.519×10^{-5} to $2.809 \times 10^{-5} \text{ A/cm}^2$. In the presence of an inhibitor, the LPR value increases and the corrosion current decreases. These results suggest that a protective film is formed on the metal surface and probably the protective film consists of Fe^{2+} inhibitor complex apart from CaCO_3 and CaO .

3.4. Implication

The extract of henna seed can be combined with concrete admixture. This combination will safeguard the mild steel that is embedded in concrete structures. This discovery may have practical applications in the field of concrete technology.

3.5. Analysis of SEM images

The analysis of SEM images has been utilized in research related to corrosion inhibition [17–21]. A significant degree of corrosion protection leads to a comparatively smooth surface of the film. The film will demonstrate uniformity [22–25].

In contrast, when the system undergoes corrosion or when the corrosion protection is insufficient, the surface becomes irregular. Pits will form. The protective layer will be inconsistent. These findings, along with an analysis of **Figure 6**, suggest that the corrosion protection of mild steel is relatively diminished in the presence of SCPS. However, when SCPS is used in conjunction with henna seed extract, the corrosion protection is enhanced.

This is consistent with the results of the electrochemical analysis, particularly the polarization examination.

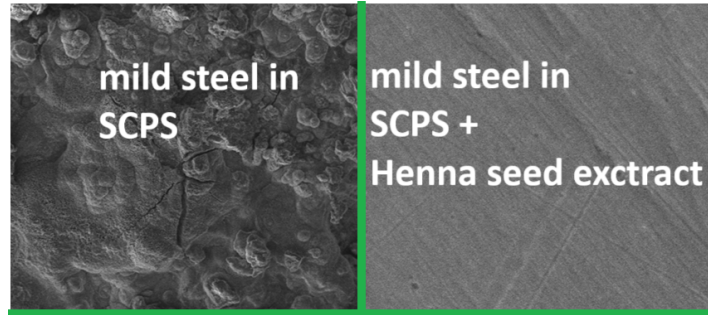


Figure 6. SEM images of various surfaces.

3.6. Analysis of contact angle measurements

Contact angle measurements have been employed in research related to corrosion inhibition [26–30]. When a surface undergoes corrosion or when its protective features are compromised, the contact angle of that surface diminishes. This leads to heightened wettability and a decrease in hydrophobicity. The water-repellent characteristics weaken. In contrast, when a surface is unaffected by corrosion or when its protective attributes are notably improved, the contact angle rises. This results in reduced wettability and an increase in hydrophobicity.

Taking into account these facts and analyzing **Figure 7**, it is clear that the presence of henna seed extract results in a significantly smoother surface of the protective film that develops on the mild steel surface when immersed in simulated concrete pore solution (SCPS). This improvement contributes to increased corrosion resistance. These results are consistent with the findings from the electrochemical study, particularly the polarization analysis, as well as the images obtained from scanning electron microscopy (SEM).

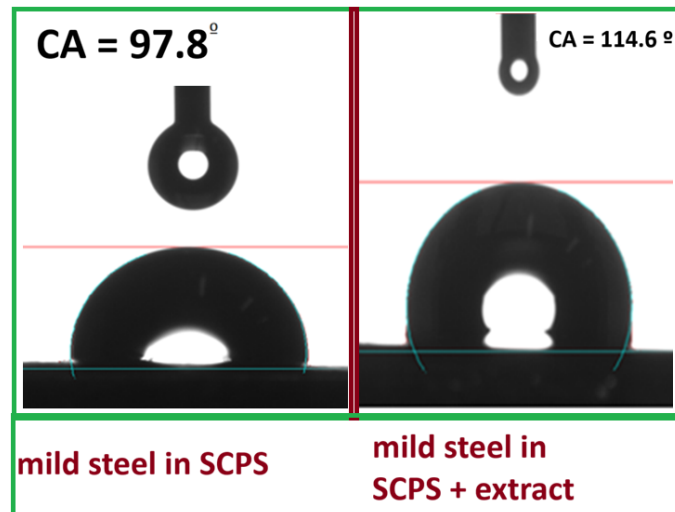


Figure 7. Contact angle measurements of various surfaces.

4. Conclusion

An aqueous extract derived from henna seed has been utilized to mitigate the corrosion of mild steel in a simulated concrete pore solution (SCPS). A polarization analysis has been conducted to assess the corrosion protection properties of the henna

seed extract (HSE).

The incorporation of henna seed extract leads to an improvement in linear polarization resistance.

At the same time, there is a decrease in the corrosion current. The transfer of electrons from the metal surface to the corrosive environment is restricted. This observation reinforces the corrosion protection offered by henna seed extract.

The surface morphology of the protective film has been examined using scanning electron microscopy (SEM). It has been observed that with the introduction of henna seed extract, the surface of the protective film appears more uniform. This further validates the protective characteristics of henna seed extract.

Such findings may have significant implications in the field of concrete technology.

A further examination of contact angle measurements reveals that the presence of henna seed extract results in a smoother texture of the protective film on the mild steel surface immersed in simulated concrete pore solution (SCPS). This improvement in smoothness is associated with enhanced corrosion resistance. These results align with the findings from the electrochemical analysis, particularly the polarization study, as well as the images obtained from scanning electron microscopy (SEM).

Author contributions: SR and AAH: concept introduced, masterminding, proofreading, editing, and writing the research article; PS and MS: designing and carrying out the experiment. All authors have read and agreed to the published version of the manuscript.

Funding: This work received no external funding.

Institutional review board statement: Not applicable.

Informed consent statement: Not applicable.

Data availability statement: Not applicable.

Acknowledgement: The authors express their gratitude to their respective managements for the assistance and support provided.

Conflict of interest: The authors declare no conflict of interest.

References

1. Carry A, Demey N, Geirinhas N. HS2 high-speed line—Supply and qualification of an electrically isolated prestressing system according to the requirements of fib 75 for a viaduct with prefabricated segments. *Proceedings of the fib Symposium*. 2025: 1595–1601.
2. Rossi D, Pettorruso C, Bruschi E, et al. Evaluation of non-destructive techniques for inspection of post-tensioned concrete bridges. *Procedia Structural Integrity*. 2024; 62: 307–314. doi: 10.1016/j.prostr.2024.09.046
3. Allady A, Maini R. Embedded Sensor Technology Application for Offshore Energy Industry. In: *Proceedings of the SNAME 28th Offshore Symposium*; 8 March 2023; Houston, TX, USA. doi: 10.5957/TOS-2023-015
4. Rymeš J, Červenka J, Pukl R. Advanced modelling of concrete structures for improved sustainability. *Acta Polytechnica CTU Proceedings*. 2022; 38: 190–195. doi: 10.14311/APP.2022.38.0190
5. Venkatesh V, Kodoth K, Jacob AA, et al. Assessment of Structural Integrity of Submerged Concrete Structures Using Quantitative Non-Destructive Techniques Deployed from Remotely Operated Underwater

- Vehicles (ROV). In: Proceedings of the OCEANS 2022; 21 February 2022; Chennai, India. pp. 1–6. doi: 10.1109/OCEANSSChennai45887.2022.9775418
6. Stoiber N, Hammerl M, Kromoser B. Cradle-to-gate life cycle assessment of CFRP reinforcement for concrete structures: Calculation basis and exemplary application. *Journal of Cleaner Production*. 2021; 280: 124300. doi: 10.1016/j.jclepro.2020.124300
 7. Ladouceur L, Cordova L, Agostini L, et al. Concrete temperature management by alternatively using post-cooling or pre-cooling (liquid nitrogen) during construction of the “Puente del Atlantico” in Panama. *Proceedings of the fib Symposium*. 2018: 1158–1170.
 8. Heffron R. Numerical Modeling to Achieve Concrete Durability for New Waterfront Structures of 100 Years or More, but at What Price? In: Proceedings of the 12th Triannual International Conference on Ports, American Society of Civil Engineers; 22 April 2010; Jacksonville, FL, USA. pp. 376–385. doi: 10.1061/41098(368)39
 9. Muñoz E, Valbuena E. State evaluation of steel bridges of the Colombian national roadway network. *Revista de la Facultad de Ingeniería*. 2016; 31(2): 462–489.
 10. Silver ES. Bridge steps lightly to spare cash crop. *Engineering News Record (Supplement)*. 2004: 14–19.
 11. Search Images—Henna seeds. Available online: <https://www.bing.com/images/search?q=henna+seeds&form=HDRSC3&first=1> (accessed on 1 November 2025).
 12. Mrayej HE, Ettahiri W, Adardour M, et al. Corrosion Inhibition of Mild Steel in Hydrochloric Acid Solution by Benzimidazole: Experimental and Theoretical Studies. *Indonesian Journal of Science and Technology*. 2025; 11(2): 265–292. doi: 10.17509/ijost.v11i2.89778
 13. Farghaly TA, Nassar S, Abdel-karim AM, et al. Corrosion Inhibition of Carbon Steel in HCl Solution Using a Novel Bis-Spiropyrazole Compound: Experimental and Quantum Calculations. *Journal of Bio- and Tribo-Corrosion*. 2026; 12(1): 2. doi: 10.1007/s40735-025-01053-1
 14. Kellal R, Wang Q, Safi ZS, et al. Rosa Damascena Extract as a Green Corrosion Inhibitor for Carbon Steel in Acidic Solutions: Experimental Findings and Computational Insights. *Journal of Bio- and Tribo-Corrosion*. 2026; 12(1): 7. doi: 10.1007/s40735-025-01071-z
 15. Youssef A, Ennafaa F, Idrhoussaine N, et al. Study of the anti-corrosion properties of a novel chloro C4-substituted heterocyclic organic pyrazolone for mild steel in HCl solution. *Journal of Molecular Structure*. 2026; 1353: 144645. doi: 10.1016/j.molstruc.2025.144645
 16. Vashisht H, Singh MR, Kathpalia R, et al. Hydrophobic alkyl-chain-modified (4-bromobutyl) triphenyl phosphonium bromide as a potential corrosion inhibitor for mild steel in Yamuna River water of India. *Journal of Molecular Structure*. 2026; 1353: 144580. doi: 10.1016/j.molstruc.2025.144580
 17. Yadav OS, Kumar S, Yadav K, et al. Investigations Properties on the Corrosion Inhibition of Kala Bansa Leaf Extract on Mild Steel in an Acidic Environment. *Portugaliae Electrochimica Acta*. 2026; 44(1): 27–45. doi: 10.4152/pea.2026440103
 18. Azogagh M, Hmada A, Barazzouq A, et al. Evaluation of novel glycidyl ether methylene phthalimide epoxy resin for mild steel corrosion inhibition in 1 M HCl: Synthesis, characterization, electrochemical, and DFT/MD comprehensive approaches. *Journal of Molecular Structure*. 2025; 1346: 143112. doi: 10.1016/j.molstruc.2025.143112
 19. Megahed MM, AbdElRhiem E, Atta W, et al. Investigation and evaluation of the efficiency of palm kernel oil extract for corrosion inhibition of brass artifacts. *Scientific Reports*. 2025; 15(1): 4473. doi: 10.1038/s41598-025-88370-0
 20. Aldahiri RH, Hussein MA, Al-Bukhari SMA, et al. Synergistic effect of *Canarium strictum* leaves extract and KI on the corrosion protection of mild steel in 15% HCl solution. *Scientific Reports*. 2025; 15(1): 3576. doi: 10.1038/s41598-025-87482-x
 21. Fouda AS, Rashwan S, Ibrahim H, et al. *Cuminum cyminum* as green corrosion inhibitor for API 5 L X70 carbon steel in 0.5 M H₂SO₄ solution. *Scientific Reports*. 2025; 15(1): 17120. doi: 10.1038/s41598-025-98407-z
 22. Raid M, El Harmouchi H, Belhadj O, et al. Investigating the effectiveness of an aromatic derivative with a calix[4]arene structure as a corrosion inhibitor for extra-mild steel in acidic medium (1 M HCl). *Hybrid Advances*. 2026; 12: 100570. doi: 10.1016/j.hybadv.2025.100570
 23. Zhao J, Yang L, Chen F, et al. Microstructure and corrosion of cold-sprayed/laser-remelted TC4 coatings on 316 L SS in oxygenated NaCl-containing super/subcritical water. *The Journal of Supercritical Fluids*. 2026; 229: 106804. doi: 10.1016/j.supflu.2025.106804
 24. Banumathi R, Syed Abuthahir SS, Mohamed Kasim Sheit H, et al. Investigation of *Baccaurea Ramiflora* Leaf Extract as Sustainable Corrosion Inhibitor for Carbon Steel in Acidic Medium. *Journal of Bio- and Tribo-Corrosion*. 2026;

- 12(1): 13. doi: 10.1007/s40735-025-01076-8
25. Shaban G, Bartawi EH, Andersson MP, et al. Effect of temperature on CO₂ corrosion inhibition by black tea extract: A combined experimental and molecular modelling study. *Materials Today Sustainability*. 2026; 33: 101271. doi: 10.1016/j.mtsust.2025.101271
 26. Punathil Meethal R, Kumar S, Yadav M, et al. Polyethyleneimine polymer as an effective corrosion inhibitor for advanced node tungsten post-CMP cleaning. *Applied Surface Science*. 2026; 716: 164670. doi: 10.1016/j.apsusc.2025.164670
 27. Liu X, Jiang L, Li Q, et al. MBT + CVL@Fe₃O₄ enhanced epoxy coating for self-healing and self-warning performance. *Progress in Organic Coatings*. 2026; 211: 109746. doi: 10.1016/j.porgcoat.2025.109746
 28. Asrafali SP, Periyasamy T, Rananavare AP, et al. Multifunctional hybrid polybenzoxazine/PEG-PPG-PEG coatings from renewable sesamol-furfurylamine benzoxazine with superior thermal, anti-fouling and corrosion resistance. *Progress in Organic Coatings*. 2026; 211: 109822. doi: 10.1016/j.porgcoat.2025.109822
 29. Habib S, Arshad S, Butt ARS, et al. A shield and a signal: Smart polymeric coatings reinforced with zinc-imidazole carboxylate framework for dual corrosion inhibition and corrosion sensing. *Journal of Colloid and Interface Science*. 2026; 703: 139293. doi: 10.1016/j.jcis.2025.139293
 30. Cai M, Mei P, Lai L. Comparative study on the corrosion inhibition performance of hydrophilic and amphiphilic carbon dots in hydrochloric acid medium. *Carbon*. 2026; 247: 121080. doi: 10.1016/j.carbon.2025.121080